Impact of Data Fusion on Real-Time Detection in Sensor Networks

Rui Tan[1] Guoliang Xing[2] Benyuan Liu[3] Jianping Wang[1]
[1]*City University of Hong Kong, HKSAR* [2]*Michigan State University, USA*
[3]*University of Massachusetts Lowell, USA*

***Abstract*—Real-time detection is an important requirement of many mission-critical wireless sensor network applications such as battlefield monitoring and security surveillance. Due to the high network deployment cost, it is crucial to understand and predict the real-time detection capability of a sensor network. However, most existing real-time analyses are based on overly simplistic sensing models (*e.g.*, the disc model) that do not capture the stochastic nature of detection. In practice, data fusion has been adopted in a number of sensor systems to deal with sensing uncertainty and enable the collaboration among sensors. However, real-time performance analysis of sensor networks designed based on data fusion has received little attention. In this paper, we bridge this gap by investigating the fundamental real-time detection performance of large-scale sensor networks under stochastic sensing models. Our results show that data fusion is effective in achieving stringent performance requirements such as short detection delay and low false alarm rates, especially in the scenarios with low signal-to-noise ratios (SNRs). Data fusion can reduce the network density by about 60% compared with the disc model while detecting any intruder within one detection period at a false alarm rate lower than 2%. In contrast, the disc model is only suitable when the SNR is sufficiently high. Our results help understand the impact of data fusion and provide important guidelines for the design of real-time wireless sensor networks for intrusion detection.**

***Keywords*-Data fusion; real-time intrusion detection; performance limits; wireless sensor networks**

I. Introduction

Wireless sensor networks (WSNs) are increasingly available for mission-critical applications such as battlefield monitoring and security surveillance. A fundamental objective of these applications is *real-time intrusion detection* that requires any unknown intruders to be detected by the network within tight deadlines. Many intrusion detection scenarios involve a large number of sensors distributed in a vast geographical area. Moreover, sensor nodes are often not accessible after deployment due to the constraints of physical environments (*e.g.*, battlefields). Therefore, it is crucial to analyze and understand the expected real-time performance of WSNs before the actual deployment.

However, we face several key challenges in analyzing the real-time performance of sensor networks for intrusion detection. First, the real-time detection performance of a sensor network is inherently affected by the uncertainties in network deployment and sensor measurement. For instance, unpredictable environmental noises can easily trigger false alarms of low-cost sensors, resulting probabilistic detection performance. Although false alarms can be suppressed by making sensors more conservative, it inevitably jeopardizes the timeliness of detection. There exist fundamental trade-offs between real-time and other detection performance metrics of a sensor network. Second, the adoption of advanced signal processing algorithms often significantly complicates the modeling and analysis of system real-time performance. Collaborative signal processing techniques such as data fusion [1] are widely employed by current sensor systems to enable the cooperation among multiple sensors with limited sensing capability. For instance, reliable intrusion detection in noisy environments requires the aggregation of readings from multiple sensors. However, such requirements often have complex impacts on the system real-time performance.

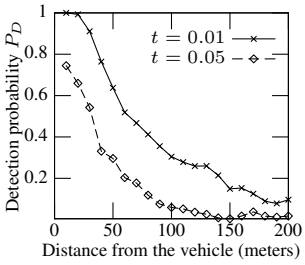

Figure 1. Detection probability *vs.* the distance from the vehicle.

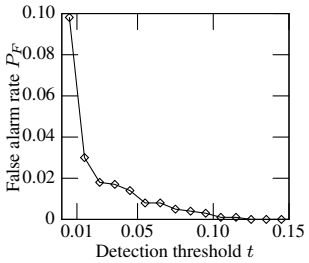

Figure 2. False alarm rate *vs.* detection threshold.

Recently, several sensor networks have been developed for real-time detection [2], [3]. However, the real-time performance of such systems are often analyzed based on *overly simplistic* sensing models [2]–[9]. In particular, the sensing region of a sensor is modeled as a disc with radius r centered at the position of the sensor, where r is referred to as the *sensing range*. A sensor *deterministically* detects the targets within its sensing range. As the simplistic disc model allows a geometric treatment to the detection problem, it has been widely adopted in the design and analysis of surveillance sensor networks. However, a key shortcoming of the disc model is that it fails to capture the stochastic nature of sensing, such as probabilistic delay and detectability caused by noise. Moreover, most studies based on the disc model do not exploit the collaboration among sensors.

To illustrate the inaccuracy of the disc model, we plot the sensing performance of an acoustic sensor in Fig. 1 and 2 using the data traces collected in a vehicle detection experiment [10]. In the experiment, the sensor detects moving vehicles by comparing its signal energy measurement against a threshold (denoted by t). Fig. 1 plots the probability that the sensor detects a vehicle (denoted by P_D) versus

the distance from the vehicle. No clear cut-off boundary between successful and unsuccessful sensing of the target can be seen in Fig. 1. Similar result is observed for the sensor's false alarm rate (denoted by P_F) and the detection threshold shown in Fig. 2. Note that P_F is the probability of making a positive decision when *no* vehicle is present.

In this work, we develop an analytical framework to study the real-time surveillance performance of large-scale WSNs that are designed based on collaborative data fusion algorithms. To quantify the fundamental trade-off between detection delay and false alarm rate, we propose a new real-time metric called α-*delay* that is defined as the delay of detecting an intruder subject to the false alarm rate bound α. The main focus of this paper is to establish the correlation between network density and α-delay in intrusion detection. We first propose a probabilistic disc model that extends the classical disc model to the context of stochastic detection. Moreover, we study the impact of data fusion on real-time detection through the comparison between the disc- and fusion-based sensing models. We show that the ratio of network densities to achieve the minimum α-delay under the two models has an asymptotic tight bound of $\Theta(\frac{\text{SNR}}{Q^{-1}(\alpha)})$, where $Q^{-1}(\cdot)$ is the inverse function of the complementary cumulative distribution function of the standard normal distribution. To the best of our knowledge, this work is the first to study the real-time performance of large-scale WSNs based on collaborative sensing models.

Our findings have several key implications for the design of real-time sensor systems for intrusion detection. First, data fusion is effective in achieving stringent performance requirements such as short detection delay and low false alarm rates, especially in the scenarios with low SNRs. Our simulations with realistic settings show that data fusion can reduce the network density by about 60% compared with the disc model while detecting any intruder within one detection period at a false alarm rate lower than 2%. Second, the disc model is suitable only when the SNR is sufficiently high. These results lay a foundation for understanding the limitation of the existing real-time analyses based on simplistic sensing models, and provide key insights into the design of fusion-based real-time surveillance WSNs.

The rest of this paper is organized as follows. Section II reviews related work. Section III introduces the preliminaries and problem definition. In Section IV and V, we derive the α-delay under the disc and fusion models, respectively. In Section VI, we study the impact of data fusion on real-time detection through performance comparison between the two models. Section VII presents simulation results and Section VIII concludes this paper.

II. Related Work

Most existing real-time analyses of target detection [4]–[6] and sensing coverage [7]–[9] in WSNs are based on the simplistic disc model. The delay of detecting a moving target with randomly deployed sensors has been analyzed in [4], [5]. The length of free path that a target travels undetected is derived in [6]. However, the disc model adopted by these works fails to capture the stochastic characteristics of real-world intrusion detection, such as probabilistic detectability and false alarms. In this paper, we study the relationship between the performance of real-time stochastic detection and network density. We propose a probabilistic disc model that naturally extends the existing analytical results [8] based on the classical disc model to the context of stochastic detection. Moreover, we study the impact of data fusion on network density and compare with the results under the probabilistic disc model.

Many sensor network systems have incorporated various data fusion schemes to improve the system performance [10]–[17]. In the surveillance system based on MICA2 motes developed in [12], the system false alarm rate is reduced by fusing the detection decisions made by multiple neighboring sensors. In the DARPA/IXOs SensIT project, advanced data fusion techniques have been employed in a number of algorithms and protocols designed for target detection [11], [13], [14], localization [15], [16], and classification [10], [17]. In our recent work, we have developed static sensor deployment algorithms [18] and mobile sensor scheduling algorithms [19]–[21] for fusion-based target detection in WSNs. However, the performance analysis of large-scale fusion-based WSNs has received little attention.

There is vast literature on stochastic signal detection based on multi-sensor data fusion. Early work [1] focuses on small-scale powerful sensor networks (*e.g.*, several radars). Recent studies on data fusion [13], [14], [22] have considered the specific properties of WSNs such as sensors' spatial distribution and limited sensing capability. However, these works focus on analyzing the optimal fusion strategies that maximize the system detection performance of a given network. Our recent work [23] investigates the fundamental impacts of data fusion on the coverage of static targets in WSNs. In contrast, this paper studies the impact of data fusion on the delay of detecting mobile targets.

III. Preliminaries and Problem Definition

In this section, we first describe the preliminaries of our work, which include sensor measurement, network, and data fusion models. We then introduce the problem definition.

A. Sensor Measurement and Network Models

Sensors perform detection by measuring the energy of signals emitted by the target. The energy of most physical signals (*e.g.*, acoustic and electromagnetic signals) attenuates with the distance from the signal source. Suppose sensor i is d_i meters away from the target that emits a signal of energy S. The attenuated signal energy s_i at the position of sensor i is given by $s_i = S \cdot w(d_i)$, where $w(\cdot)$ is a decreasing function satisfying $w(0) = 1$ and $w(\infty) = 0$. The $w(\cdot)$ is

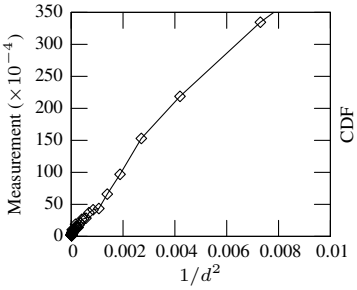

Figure 3. Energy measurement *vs.* $1/d^2$ (d is the distance from the target, in the unit of meters).

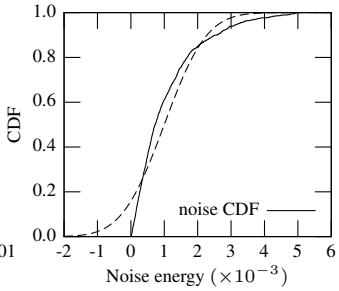

Figure 4. The CDF of noise energy. The dashed line is the CDF of $\mathcal{N}(0.001, 0.001^2)$.

referred to as the *signal decay function*. In this paper, we assume $w(d) = 1/(1+d^2)$. Such a model avoids singularity when d is close to zero and approximates the inverse-square law [16], [24] when d is large.

The measurements of sensors are contaminated by additive random noises from sensor hardware or environment. Depending on the hypothesis that the target is absent (H_0) or present (H_1), the measurement of sensor i, denoted by y_i, is given by

$$H_0 : y_i = n_i,$$
$$H_1 : y_i = s_i + n_i,$$

where n_i is the energy of noise experienced by sensor i. We assume that the noise n_i at each sensor i follows the normal distribution, *i.e.*, $n_i \sim \mathcal{N}(\mu, \sigma^2)$, where μ and σ^2 are the mean and variance of n_i, respectively. We assume that the noises, $\{n_i|\forall i\}$, are spatially independent across sensors. Therefore, the noises at sensors are independent and identically distributed (*i.i.d.*) Gaussian noises. In the presence of target, the measurement of sensor i follows the normal distribution, *i.e.*, $y_i|H_1 \sim \mathcal{N}(s_i + \mu, \sigma^2)$. Due to the independence of noises, the sensors' measurements, $\{y_i|\forall i, H_1\}$, are spatially independent but *not* identically distributed as sensors receive different signal energies from the target. We define the SNR as $\delta = S/\sigma$ which quantifies the noise level.

The above signal decay and sensor measurement models have been widely assumed in the literature of signal detection [1], [15] and also have been empirically verified [16], [24]. Fig. 3 and Fig. 4 plot the energy of signal from driving vehicles and noise measured by an acoustic sensor in the SensIT experiments [10]. From Fig. 3, we can see that the signal energy increases linearly with $1/d^2$, which indicates that $w(d)$ has an order of $1/d^2$. This is consistent with the signal decay model adopted in this paper. Fig. 4 plots the cumulative distribution function (CDF) of noise energy, which matches the CDF of the normal distribution $\mathcal{N}(0.001, 0.001^2)$.

We assume that a sensor executes detection task every T seconds. T is referred to as the *detection period*. In each detection period, a sensor gathers the signal energy during the *sampling interval* for the detection made in the current period. The temporal view of a single sensor's operation is illustrated in Fig. 5. We note that such an intermittent measurement scheme is consistent with several wireless sensor systems for target detection and tracking [10], [12], [13]. For instance, a sensor may wake up every 5 seconds and sample acoustic energy for 0.05 seconds, where T is 5 s and the sampling interval is 0.05 s [10]. We assume that the sampling interval is much shorter than the detection period.

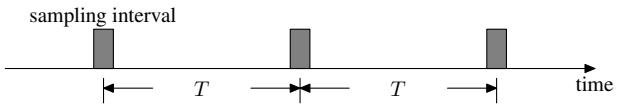

Figure 5. Temporal view of a single sensor's operation. The sensor outputs an energy measurement after each sampling interval.

We consider a network deployed in a vast two-dimensional geographical region. Several recent projects have demonstrated the deployment of large-scale sensor networks. In the ExScal project [3], [25], about 1200 nodes are distributed in an area of 1.3 km by 300 m. We assume that the positions of sensors are uniformly and independently distributed in the deployment region. Such a deployment scenario can be modeled as a stationary two-dimensional Poisson point process. Let ρ denote the density of the underlying Poisson point process. We note that such a deployment model has been widely assumed to analyze the performance of large-scale sensor networks [4]–[8]. Adopting this model thus allows us to directly compare our results with the existing results.

We assume that the target may appear at any location in the deployment region and move freely. Moreover, the target is blind to the network, *i.e.*, the target does not know the sensors' positions, and hence it cannot choose a moving scheme to reduce the probability of being detected. The sensors synchronously detect the target, and we refer to the target detection in one detection period as the *unit detection*. The process of detecting a target consists of a series of unit detections. As the sampling interval is much shorter than the detection period, we ignore the target's movement during the sampling interval.

Table I summarizes the notation used in this paper.

B. Data Fusion Model

Data fusion [1] can improve the performance of detection systems by jointly considering the noisy measurements of multiple sensors. There exist two basic data fusion schemes, namely, *decision fusion* and *value fusion*. In decision fusion [22], each sensor makes a local decision based on its measurement and sends its decision to the cluster head, which makes a system decision according to the local decisions. In value fusion [14], each sensor sends its energy measurements to the cluster head, which makes a decision based on the measurements. In this paper, we focus on value fusion, as it usually has better detection performance than decision

Table I
SUMMARY OF NOTATION

Symbol	Definition
S	original energy emitted by the target
μ, σ^2	mean and variance of noise energy
δ	signal-to-noise ratio (SNR), $\delta = S/\sigma$
d_i	distance from the target
$w(\cdot)$	signal decay function, in this paper, $w(d) = \frac{1}{1+d^2}$
s_i	attenuated signal energy, $s_i = S \cdot w(d_i)$
n_i	noise energy, $n_i \sim \mathcal{N}(\mu, \sigma^2)$
H_0 / H_1	hypothesis that the target is absent / present
y_i	energy measurement, $y_i \vert H_0 = n_i$, $y_i \vert H_1 = s_i + n_i$
α	upper bound of false alarm rate
ρ	network density
$\mathbf{F}(P)$	the set of sensors within fusion range of point P
$N(P)$	the number of sensors in $\mathbf{F}(P)$

* The symbols with subscript i refer to the notation of sensor i.

fusion [1]. As proved in [23], the optimal value fusion rule is to compare the weighted sum of measurements, $\sum_i \frac{s_i}{\sigma} \cdot y_i$, against a threshold. However, as the measurements contain both noise and signal energy, the weight $\frac{s_i}{\sigma}$, *i.e.*, the received SNR of sensor i, is often unknown in practice. A practical solution is to adopt equal constant weights for all sensors' measurements [14], [22], [23]. Since the measurements from different sensors are treated equally, the sensors far away from the target should be excluded from data fusion as their measurements suffer low received SNRs. Therefore, we adopt a fusion scheme as follows.

For any physical point P, the sensors within a distance of R meters from P participate in the data fusion to detect whether a target is present at P. R is referred to as the *fusion range* and $\mathbf{F}(P)$ denotes the set of sensors within the fusion range of P. The number of sensors in $\mathbf{F}(P)$ is represented by $N(P)$. For conciseness, we use $\mathbf{F}$ for $\mathbf{F}(P)$ and N for $N(P)$ when the point of interest is clear. Due to the Poisson process deployment, for a random point P, N follows the Poisson distribution with mean of $\rho\pi R^2$, *i.e.*, $N \sim \text{Poi}(\rho\pi R^2)$. In each detection period, a cluster head is elected to make the detection decision by comparing the sum of measurements reported by member sensors within the fusion range against a detection threshold η. Let Y denote the sum of measurements, *i.e.*, $Y = \sum_{i \in \mathbf{F}} y_i$. If $Y \geq \eta$, the cluster head decides H_1; otherwise, it decides H_0. Fig. 6 illustrates the intrusion detection under the data fusion model.

We assume that the system can obtain the position of a possible target through a localization service in the network [15], [16]. Our previous analysis [26] based on a simple localization algorithm shows that the localization error decreases with network density and becomes insignificant when the network density is high enough. Under such an assumption, the localization error can be safely ignored in our analysis that is focused on the detection delay when the network density is high. We also evaluate the impact of localization error through simulations in Section VII.

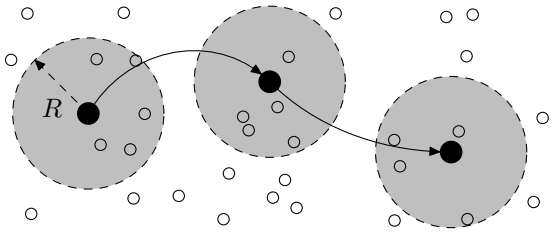

Figure 6. Intrusion detection under data fusion model. The void circles represent randomly deployed sensors; the solid circles represent the target in different sampling intervals, and a unit detection is performed in each sampling interval; the dashed discs represent the fusion ranges.

In each detection period, a cluster is formed by the sensors within the fusion range centered at the possible target to make a detection decision. The cluster formation may be initiated by the sensor that has the maximum measurement. Such a scheme can be implemented by several dynamic clustering algorithms [27]. The fusion range R can be used as an input parameter of the clustering algorithm.

C. Problem Definition

In this paper, we study the delay of stochastic intrusion detection in large-scale sensor networks. As the process of detecting a target is inherently stochastic, the detection delay is closely related to two system performance metrics, namely, the false alarm rate (denoted by P_F) and detection probability (denoted by P_D). P_F is the probability of making a positive decision when no target is present, and P_D is the probability that a present target is correctly detected. In stochastic detection, positive detection decisions may be false alarms caused by the noise in sensor measurements. Note that the false alarm rate does not depend on the property of target as it is the probability of making positive decision when *no* target is present. Although detection delay can be reduced by setting lower detection thresholds, the fidelity of detection results may be unacceptable because of high false alarm rates. Therefore, studying detection delay alone without the consideration of false alarm is meaningless. We now introduce a concept called α-*delay* that quantifies the delay of detection under bounded false alarm rate.

Definition 1. α-delay is the average number of detection periods before a target is first detected subject to that the false alarm rate of the network is no greater than α, *i.e.*, $P_F \leq \alpha$, where $\alpha \in (0, 1)$.

In practice, mission-critical surveillance applications require a low false alarm rate ($\alpha < 5\%$) [12], [28], as false alarms not only reduce the fidelity of detection results but also waste energy in responsive operations such as wakening asleep sensors. The focus of this paper is to study the relationship between the α-delay and network density. Network density directly determines the cost of constructing and deploying a network. Thus, our results will allow the

network designer to achieve desirable trade-offs between cost, false alarm rate, and detection delay. Moreover, many sensor networks reduce energy consumption by only activating a subset of nodes while scheduling others to sleep [12]. Our results can be applied to reduce the density of active nodes while achieving the required detection delay. As the detection delay often dominates the communication delay in stochastic intrusion detection, we ignore the communication delay in this paper. For instance, the delay of aggregating the readings of a group of nodes is within 5 milliseconds [2] while the detection period can be several seconds.

We address the following problems in this paper:

1) Are the analytical results on detection delay [4]–[9] derived under the classical disc model still applicable under the definition of α-delay? We propose a probabilistic disc model such that the existing results can be naturally extended to the context of stochastic detection (Section IV).
2) How to quantify the α-delay when sensors can collaborate through data fusion? Answering this question enables us to evaluate the timeliness of a fusion-based network and to deploy or turn on the fewest sensors for achieving a given α-delay (Section V).
3) What is the impact of data fusion on network density when the α-delay is minimized? Many mission-critical real-time applications require detection delay to be as short as possible [12], [28]. We analytically compare the network densities under the disc and fusion models when the α-delay is minimized. The result provides important insights into understanding the limitation of the disc model and the impact of data fusion on the design of real-time WSNs (Section VI).

IV. α-Delay under Probabilistic Disc Model

In the classical disc model, each sensor has deterministic sensing capability within its sensing range. If the target is within at least one sensor's sensing range, the target is regarded to be detected by the network. Such a model is not consistent with the stochastic nature of signal detection. As a result, although a number of studies [4]–[9] have been conducted on intrusion detection based on the disc model, they cannot be readily used to analyze the performance or guide the design of real-world intrusion detection systems. In this section, we extend the classical disc model based on the stochastic detection theory [1] to capture several realistic sensing characteristics and study the α-delay under the extended model. The result lays a foundation for understanding the limitation of disc model on quantifying the delay of intrusion detection.

A. Probabilistic Disc Model

In the *probabilistic disc model*, we choose sensing range r such that 1) the probability of detecting any target within r meters from it is no lower than β, and 2) the false alarm rate is no greater than α, where α and β are parameters specified by user. Note that α and β are both within $(0, 1)$. As we ignore the detection probability outside the sensing range of a sensor, the detection capability of sensor under this model is lower than in reality. However, this model preserves the *boundary* of sensing region defined in the classical disc model. Accordingly, the existing analytical results based on the classical model [4]–[9] can be naturally extended to the context of stochastic detection. In Section IV-B, we will discuss how to extend the coverage probability derived under the classical model [8] to study the α-delay of stochastic intrusion detection.

We now discuss how to choose the sensing range r under the probabilistic disc model. The optimal Bayesian detection rule for a single sensor i is to compare its measurement y_i against a detection threshold t [1]. If y_i exceeds t, sensor i decides H_1; otherwise, it decides H_0. As both $y_i|H_0$ and $y_i|H_1$ follow the normal distributions, *i.e.*, $y_i|H_0 = n_i \sim \mathcal{N}(\mu, \sigma^2)$ and $y_i|H_1 = s_i + n_i \sim \mathcal{N}(\mu + s_i, \sigma^2)$, the false alarm rate and detection probability of sensor i are given by

$$P_F = \mathbb{P}(y_i \geq t|H_0) = Q\left(\frac{t-\mu}{\sigma}\right), \tag{1}$$

$$P_D = \mathbb{P}(y_i \geq t|H_1) = Q\left(\frac{t-\mu-s_i}{\sigma}\right), \tag{2}$$

where $Q(\cdot)$ is the complementary CDF of the standard normal distribution, formally, $Q(x) = \frac{1}{\sqrt{2\pi}}\int_x^\infty \mathrm{e}^{-t^2/2}\mathrm{d}t$. To derive the sensing range, we let $P_F = \alpha$ and $P_D = \beta$. The detection threshold t can then be solved from (1) as $t = \mu + \sigma Q^{-1}(\alpha)$, where $Q^{-1}(\cdot)$ is the inverse function of $Q(\cdot)$. Moreover, by replacing $s_i = S \cdot w(r)$ in (2), we have

$$r = \sqrt{\frac{\delta}{Q^{-1}(\alpha) - Q^{-1}(\beta)} - 1}. \tag{3}$$

For instance, the sensing range r is 3.8 m if $\alpha = 0.05$, $\beta = 0.95$ and $\delta = 50$ (*i.e.*, 17 dB).[1] Moreover, we can see from (3) that r increases with the SNR δ. This conforms to the intuition that a sensor can detect a farther target if the noise level is lower (*i.e.*, a greater δ). As $Q^{-1}(\cdot)$ is a decreasing function, r will decrease if a lower false alarm rate is required (*i.e.*, a smaller α).

B. α-Delay under Probabilistic Disc Model

The intrusion detection under the probabilistic disc model works as follows. The network periodically detects the target as described in Section III-C. In each unit detection, if the target is within at least one sensor's sensing range, the target is detected with a probability no lower than β. We let β be sufficiently close to 1 (*e.g.*, $\beta = 0.99$) such that the target is detected almost surely if it is within any sensor's sensing range. Such a setting enables the sensors to exhibit similar

[1] The SNR is set to be 17 dB according to the measurements in the vehicle detection experiments based on MICA2 [29] and ExScal [25] motes.

deterministic property as under the classical disc model. We refer to the circular region with radius of r centered at the target as the *target disc*. Hence, the target is detected if there is at least one sensor within the target disc. We have the following lemma.

Lemma 1. *If there is no overlap between any two target discs, the α-delay under the probabilistic disc model is $\tau = 1/(1-\mathrm{e}^{-\rho\pi r^2})$.*

Proof: As shown in [8], when the sensors are deployed according to the Poisson process, the probability that there is at least one sensor in a target disc is $p = 1-\mathrm{e}^{-\rho\pi r^2}$. Suppose the target is detected in the J^{th} ($J \geq 1$) detection period. As there is no overlap between any two target discs, the unit detections are independent from each other. Therefore, J follows the geometric distribution with a success probability of p in each Bernoulli trial (*i.e.*, each unit detection). Moreover, according to the definition of r in (3), the false alarm rate in each unit detection is no greater than α. According to Definition 1, the α-delay is given by $\tau = \mathbb{E}[J] = \frac{1}{p} = \frac{1}{1-\mathrm{e}^{-\rho\pi r^2}}$. ■

We can see from Lemma 1 that the α-delay decreases with network density ρ and sensing range r. Note that r is given by (3) under the probabilistic disc model. In this paper, we focus on the case where there is no overlap among target discs. This condition can easily hold in practice. For instance, if the sensing range r is 3.8 m as mentioned in Section IV-A and the target moves at a constant speed of 5 m/s (*i.e.*, 18 km/h) [10], the target disc will not overlap as long as the detection period T is greater than 2 s.

V. α-Delay under Data Fusion Model

Although the probabilistic disc model discussed in Section IV captures the stochastic nature of sensing, it does not exploit the possible collaboration among sensors. In this section, we derive the detection performance and α-delay under the data fusion model presented in Section III-B.

A. Performance Modeling of Fusion-based Detection

In this section, we derive the false alarm rate and detection probability in a unit detection. The results will be used in Section V-B to analyze the α-delay under the fusion model.

When no target is present, each sensor measures *i.i.d.* noise as discussed in Section III-A. Denote $\mathbf{F}_j$ as the set of sensors within the fusion range in the j^{th} unit detection. Suppose there are N_j sensors in $\mathbf{F}_j$. The sum of energy measurements follows the normal distribution, *i.e.*, $Y|H_0 = \sum_{i\in\mathbf{F}_j} n_i \sim \mathcal{N}(N_j\mu, N_j\sigma^2)$. Therefore, the false alarm rate of the j^{th} unit detection is given by $P_{Fj} = \mathbb{P}(Y \geq \eta|H_0) = Q\left(\frac{\eta - N_j\mu}{\sqrt{N_j}\sigma}\right)$, where η is the detection threshold. As P_D is a non-decreasing function of P_F [1], it is maximized when P_F is set to be the upper bound α. Such a scheme is referred to as the constant false alarm rate detector [1]. Let $P_{Fj} = \alpha$, the optimal detection threshold can be derived as $\eta^* = N_j\mu + \sqrt{N_j}\sigma Q^{-1}(\alpha)$.

When the target is present, the sum of energy measurements in the j^{th} unit detection is $Y|H_1 = \sum_{i\in\mathbf{F}_j} s_i + \sum_{i\in\mathbf{F}_j} n_i$. The attenuated signal energies $\{s_i|i \in \mathbf{F}_j\}$ are *i.i.d.* and we denote μ_s and σ_s^2 as the mean and variance of s_i, respectively. The proof for the independence of $\{s_i|i \in \mathbf{F}_j\}$ and the derivation of μ_s and σ_s^2 can be found in Appendix A. Note that both μ_s and σ_s^2 are determined by the target energy S, the signal decay function $w(d)$ and fusion range R. If N_j is large enough, $\sum_{i\in\mathbf{F}_j} s_i$ approaches the normal distribution according to the central limit theorem, *i.e.*, $\sum_{i\in\mathbf{F}_j} s_i \sim \mathcal{N}(N_j\mu_s, N_j\sigma_s^2)$. As the sum of two independent Gaussians is also Gaussian, $Y|H_1$ follows the normal distribution, *i.e.*, $Y|H_1 \sim \mathcal{N}(N_j\mu_s + N_j\mu, N_j\sigma_s^2 + N_j\sigma^2)$. Hence, the detection probability in the j^{th} unit detection is given by $P_{Dj} = \mathbb{P}(Y \geq \eta|H_1) \simeq Q\left(\frac{\eta - N_j\mu_s - N_j\mu}{\sqrt{N_j}\cdot\sqrt{\sigma_s^2+\sigma^2}}\right)$. By replacing η with the optimal detection threshold η^*,

$$P_{Dj} \simeq Q\left(\frac{\sigma}{\sqrt{\sigma_s^2+\sigma^2}}\cdot Q^{-1}(\alpha) - \frac{\mu_s}{\sqrt{\sigma_s^2+\sigma^2}}\cdot\sqrt{N_j}\right). \quad (4)$$

B. α-Delay of Fusion-based Detection

As discussed in Section III-C, the process of detecting a target consists of a series of unit detections. Based on the performance modeling of each unit detection in Section V-A, we now derive the α-delay under the data fusion model.

We assume that there is no common sensor between any two fusion ranges (as shown in Fig. 6). As a result, the sensor sets $\{\mathbf{F}_j|j \geq 1\}$ are independent. If the target moves along a straight line at a constant speed of v, the condition for this case can be derived as $vT \geq 2R$. We note that this condition can easily hold in practice. For instance, if the fusion range R is set to be 10 m and the target moves at a constant speed of 5 m/s (*i.e.*, 18 km/h) [10], no two fusion ranges will overlap as long as the detection period T is greater than 4 s.

From (4), P_{Dj} is a function of N_j. When the sensor sets $\{\mathbf{F}_j|j \geq 1\}$ are independent, $\{P_{Dj}|j \geq 1\}$ are *i.i.d.* as the numbers of sensors involved in each unit detection (*i.e.*, $\{N_j|j \geq 1\}$) are *i.i.d.* due to the Poisson process. We denote $\mathbb{E}[P_D]$ as the mean of P_{Dj} for any j, *i.e.*, $\mathbb{E}[P_D] = \mathbb{E}[P_{Dj}]$, $\forall j$. Intuitively, the intrusion detection can be viewed as a series of infinite Bernoulli trials and the success probability of each Bernoulli trial is $\mathbb{E}[P_D]$. Accordingly, the number of unit detections before (and including) the first successful unit detection follows the geometric distribution with a mean of $1/\mathbb{E}[P_D]$. Hence the α-delay is given by the following theorem (the formal proof is omitted due to space limitation and can be found in [26]).

Theorem 1. *The α-delay of fusion-based detection is $\tau = 1/\mathbb{E}[P_D]$, where $\mathbb{E}[P_D]$ is the average detection probability*

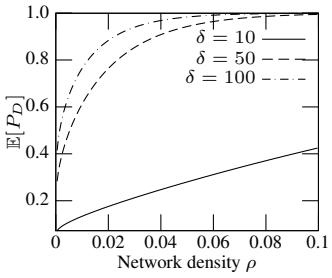

Figure 7. Mean detection probability *vs.* network density ($R = 25\,\mathrm{m}$).

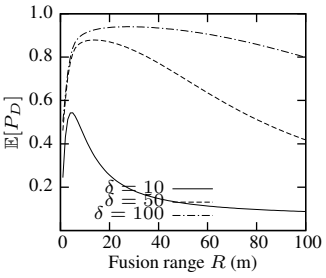

Figure 8. Mean detection probability *vs.* fusion range ($\rho = 0.03$).

in any unit detection.

We now discuss how to compute $\mathbb{E}[P_D]$ in Theorem 1. As P_{Dj} is a function of N_j and N_j follows the Poisson distribution, *i.e.*, $N_j \sim \mathrm{Poi}(\rho\pi R^2)$, $\mathbb{E}[P_D]$ is given by

$$\mathbb{E}[P_D] = \sum_{N_j=0}^{\infty} P_{Dj} \cdot f_{\mathrm{Poi}}(N_j|\rho\pi R^2), \tag{5}$$

where $f_{\mathrm{Poi}}(k|\lambda)$ is the probability density function (PDF) of the Poisson distribution $\mathrm{Poi}(\lambda)$. Specifically, $f_{\mathrm{Poi}}(k|\lambda) = \lambda^k \mathrm{e}^{-\lambda}/k!$. Note that P_{Dj} in (5) is computed using (4).

Fig. 7 and Fig. 8 plot $\mathbb{E}[P_D]$ versus network density ρ and fusion range R, respectively. From Fig. 7, we can see that $\mathbb{E}[P_D]$ increases with ρ. Moreover, for a certain ρ, $\mathbb{E}[P_D]$ increases with the SNR. From Fig. 8, we can see that $\mathbb{E}[P_D]$ is a concave function of fusion range R and there exists an optimal R that maximizes $\mathbb{E}[P_D]$. Intuitively, as the fusion range initially increases, more sensors contribute to the data fusion resulting in better sensing quality. However, as the fusion range becomes very large, the aggregate noise starts to cancel out the benefit because the target signal decreases rapidly with the distance from the target. In other words, the measurements of sensors far away from the target contain low-quality information and hence fusing them lowers detection performance. In practice, we can choose the optimal fusion range according to numerical results.

VI. Impact of Data Fusion on Real-Time Detection

Many mission-critical real-time applications require detection delay to be as small as possible [12], [28]. As an asymptotic case, the α-delay approaches one, *i.e.*, any intruder can be detected almost surely in the first detection period after its appearance, which is referred to as the *instant detection*. As a smaller detection delay always requires more sensors, the network density for achieving instant detection is an important cost metric for mission-critical real-time sensor networks.

In this section, we investigate the required network density for achieving instant detection under both the disc and fusion models. According to Lemma 1 and Theorem 1, the network density under both models approaches infinity when the α-delay reduces to one. However, the speed that the network density increases is different. In this section, we study the ratio of network densities for instant detection under the two models, which characterize the relative cost of the two models when detection delay is minimized. The result provides important insights into understanding the limitation of the disc model and the impact of data fusion on the performance of real-time WSNs for intrusion detection.

A. Network Density for Achieving Instant Detection

We abuse the symbols a bit to use N instead of N_j and P_D instead of P_{Dj} as we are not interested in the index of unit detection. As $\rho \to \infty$, $N \to \infty$ almost surely. In (4), the second item $-\frac{\mu_s}{\sqrt{\sigma_s^2+\sigma^2}} \cdot \sqrt{N}$ dominates when $\rho \to \infty$, since the first item $\frac{\sigma}{\sqrt{\sigma_s^2+\sigma^2}} \cdot Q^{-1}(\alpha)$ is a constant. Therefore, it's safe to use $P_D = Q(k\sqrt{N})$ to approximate (4), where $k = -\frac{\mu_s}{\sqrt{\sigma_s^2+\sigma^2}}$. We have the following lemma.

Lemma 2. *Let ρ_f and ρ_d denote the network densities for achieving α-delay of τ under the fusion and disc models, respectively. There exists $\xi \in (0,1)$ such that*

$$\frac{2}{k^2R^2} \cdot r^2 \le \lim_{\tau \to 1^+} \frac{\rho_f}{\rho_d} \le \frac{2}{\xi k^2 R^2} \cdot r^2. \tag{6}$$

The proof can be found in Appendix B. Note that ξ is a function of k (given by (10)). According to Lemma 2, $\lim_{\tau\to 1^+} \rho_f/\rho_d$ is largely affected by the sensing range of a single sensor. According to (3), the sensing range r is determined by the requirements on false alarm rate and detection probability (*i.e.*, α and β), as well as the SNR δ. As discussed in Section IV-B, β is a constant close to one. Accordingly, we only analyze the impacts of α and δ on the network density for achieving instant detection. We have the following theorem.

Theorem 2. *The ratio of network densities for instant detection under the fusion and disc models has an asymptotic tight bound of*

$$\lim_{\tau \to 1^+} \frac{\rho_f}{\rho_d} = \Theta\left(\frac{\delta}{Q^{-1}(\alpha)}\right). \tag{7}$$

Proof: In Lemma 2, k depends on the SNR δ, *i.e.*,

$$k = -\frac{\mu_s}{\sqrt{\sigma_s^2+\sigma^2}} = -\frac{S\mu_0}{\sqrt{S^2\sigma_0^2+\sigma^2}} = -\frac{\mu_0}{\sqrt{\sigma_0^2+\frac{1}{\delta^2}}},$$

where μ_0 and σ_0^2 (both defined in Appendix A) are constants. Moreover, ξ is a function of k (given by (10)). Accordingly, k and ξ are both constants when δ is fixed or approaches infinity. Hence, according to Lemma 2, the tight bound of the density ratio is $\lim_{\tau\to 1^+} \rho_f/\rho_d = \Theta(r^2)$. From (3), for fixed β, $r^2 = \Theta(\delta/Q^{-1}(\alpha))$. Therefore, we have (7). ∎

Theorem 2 suggests that the relative cost for instant detection between the fusion and disc models depends on the required false alarm rate α and SNR δ. Specifically, for a fixed SNR, when $\alpha \to 0$, $Q^{-1}(\alpha) \to \infty$ and hence

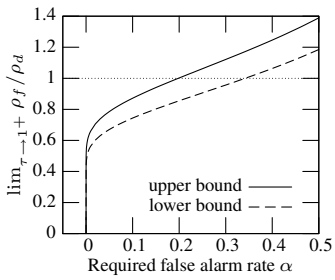

Figure 9. Density ratio *vs.* required false alarm rate ($\delta = 50$, $R = 37$ m).

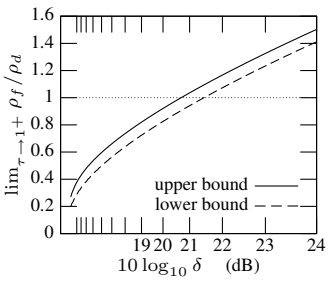

Figure 10. Density ratio *vs.* SNR ($\alpha = 0.01$).

$\lim_{\tau\to 1^+} \rho_f/\rho_d \to 0$. This suggests that the data fusion model can significantly reduce the network density when a small false alarm rate is required. Moreover, for a fixed false alarm rate, $\lim_{\tau\to 1^+} \rho_f/\rho_d$ increases with δ. That is, the advantage of data fusion diminishes as the SNR increases.

B. Application of Results

In this section, we use two realistic examples to illustrate the implications of Theorem 2. They also provide several important insights into understanding the applicability of the disc model and the data fusion model in various application scenarios.

1) Data fusion reduces network density: As discussed in Section VI-A, $\lim_{\tau\to 1^+} \rho_f/\rho_d$ decreases to zero when $\alpha \to 0$. If a small α is required, $\rho_f < \rho_d$ for instant detection, *i.e.*, the fusion model requires lower network density than the disc model. In other words, data fusion is effective in reducing detection delay and false alarms. Fig. 9 plots the lower and upper bounds of the density ratio given by Lemma 2. We set the SNR δ to be 50 (*i.e.*, 17 dB) according to the measurements in the vehicle detection experiments based on MICA2 [29] and ExScal [25] motes. The fusion range R is optimized to be 37 m. From the figure, we can see that if $\alpha < 0.2$, the fusion model will outperform the disc model. In practice, most mission-critical surveillance systems require a small α. For example, in the vehicle detection system [12] and the acoustic shooter localization system [28], the false alarm rates are tuned to be near zero.

2) Disc model suffices for high-SNR detection: As discussed in Section VI-A, for a fixed α, $\lim_{\tau\to 1^+} \rho_f/\rho_d$ increases with δ. If the SNR is high enough so that $\lim_{\tau\to 1^+} \rho_f/\rho_d > 1$, the disc model is superior to the fusion model in achieving instant detection. This implies that the disc model suffices when the SNR is high. Fig. 10 plots the bounds of density ratio given by Lemma 2. We set α to be 0.01. The fusion range R is optimized for each δ. From the figure, we can see that if the SNR is higher than 21 dB, the disc model outperforms the fusion model. Intuitively, by taking advantage of collaborative sensing, the fusion model is effective when the SNR is low to moderate. However, when the SNR is high, the detection performance of a single sensor is satisfactory and the collaboration among multiple sensors may be unnecessary.

In real systems, the noise experienced by a sensor comes from various sources, *e.g.*, the random disturbances in the environment and the electronic noise in the sensor's circuit. Thus the SNR depends on the characteristics of targets, the environment, and the sensor device. In the vehicle detection experiments based on low-power motes, *e.g.*, MICA2 [29] and ExScal [25], the SNRs are usually low to moderate ($\leq$ 17 dB). In such a case, data fusion can effectively reduce the network density required to achieve short detection delay and low false alarm rate.

VII. Performance Evaluation

In this section, we conduct simulations to evaluate the theoretical results in previous sections. We first describe the simulation settings and methodology in Section VII-A, then present the simulation results in Section VII-B.

A. Simulation Settings and Methodology

Both the mean and variance of the noise (*i.e.*, μ and σ^2) are set to be 1. The SNR δ is set to be 50 (*i.e.*, 17 dB) according to the measurements in the vehicle detection experiments based on motes [25], [29]. The fusion range R is set to be 25 m.

The sensors are deployed uniformly into a large field and periodically detect the target. The target initially appears at the origin, and moves along the X-axis at a speed of $2R$ per detection period. In the simulations, we consider the target localization error as follows. Suppose the real target position is at $P(x, y)$ when sensors take measurements, while the target position localized by the network is at $P'(x+\epsilon\cos\theta, y+\epsilon\sin\theta)$, where ϵ is a specified constant and θ is picked uniformly from $[0, 2\pi)$. Sensors within the fusion range centered at P' fuse their measurements and make the detection decision. We conduct 500 runs with different random sensor deployments. The α-delay is computed as the average number of detection periods before the target is first detected in each run.

For the disc model, the sensing range r is computed according to (3). Once the target enters the sensing range of a sensor, the sensor makes a detection decision by comparing its measurement against the detection threshold t derived in Section IV-A.

B. Simulation Results

We first evaluate the analytical result on the α-delay of fusion-based detection. Fig. 11 plots the α-delay versus the network density. The curve labeled with "analytical" plots the α-delay computed according to Theorem 1 and Eq. (5). The data points labeled with "SIM(ϵ)" represent the simulation results with a constant localization error ϵ. From the figure, we can see that the α-delay decreases with the network density. The simulation result without

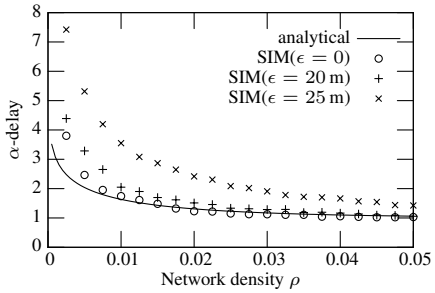

Figure 11. α-delay *vs.* network density under data fusion model.

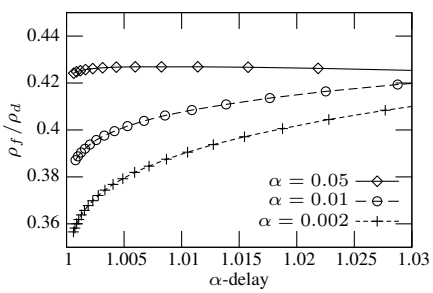

Figure 12. Density ratio *vs.* α-delay given different required false alarm rate.

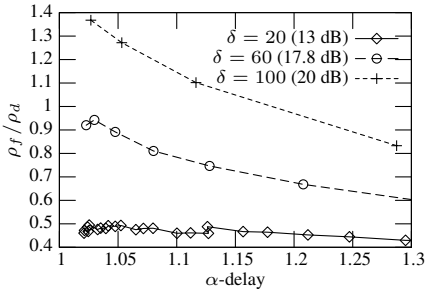

Figure 13. Density ratio *vs.* α-delay given different SNRs ($\alpha = 0.05$).

localization error (*i.e.*, $\epsilon = 0$) confirms the analytical result when the network density is greater than 0.01. When ρ is smaller than 0.01, the simulation result starts to deviate from the analytical result. This is due to the approximation made in the derivation of P_D in Section V-A. However, we can see that the maximum error between the analytical and simulation results falls within one detection period. Fig. 11 also shows that the impact of localization error is small. The simulation result has a considerable deviation from the analytical result only when the localization error is equal to the fusion range ($25\,\mathrm{m}$). In such a case, the target falls completely outside of the fusion range. Moreover, the impact of localization error diminishes as the network density increases. This result demonstrates the robustness of our analysis with respect to localization error, especially in achieving instant detection.

Fig. 12 plots the ratio of network densities required by the fusion and disc models (*i.e.*, ρ_f and ρ_d) to achieve the same α-delay, given different required false alarm rates. For instance, if the required false alarm rate is 0.05, the density ratio ρ_f/ρ_d is about 0.42 when the α-delay approaches one. This means that the disc model requires more than twice sensors for instant detection, compared with the fusion model. We can also see that $\lim_{\tau \to 1^+} \rho_f/\rho_d$ decreases if a lower false alarm rate is required. This is consistent with our analysis in Section VI-A.

Fig. 13 plots the density ratio versus α-delay given different SNRs. We can see from the figure that the density ratio increases with the SNR. For instance, if the SNR δ is 20, the density ratio ρ_f/ρ_d is about 0.5 when the α-delay reduces to one. However, if δ increases to 100, ρ_f/ρ_d is about 1.4, which means that the disc model requires less sensors than the fusion model. This is consistent with our analysis in Section VI-A.

VIII. Conclusion

In this paper, we study the impact of data fusion on real-time detection in WSNs through the performance comparison between the disc model and data fusion model. Our results show that data fusion is effective in achieving stringent performance requirements such as short detection delay and low false alarm rate, especially in the severe scenarios with low SNRs. However, the disc model may suffice only when the SNR is sufficiently high. Our results help understand the applicability of the disc and data fusion models, and hence provide important guidelines for the design of real-time WSNs for intrusion detection.

Acknowledgment

The work described in this paper was supported by grants from the Research Grants Council of the Hong Kong Special Administrative Region, China (Project No. CityU 122307, Project No. CityU 121107).

References

[1] P. Varshney, *Distributed Detection and Data Fusion*. Spinger, 1996.

[2] T. He, P. A. Vicaire, T. Yan, L. Luo, L. Gu, G. Zhou, R. Stoleru, Q. Cao, J. A. Stankovic, and T. Abdelzaher, "Achieving real-time target tracking using wireless sensor networks," in *RTAS*, 2006.

[3] S. Bapat, V. Kulathumani, and A. Arora, "Analyzing the yield of ExScal, a large-scale wireless sensor network experiment," in *ICNP*, 2005.

[4] Q. Cao, T. Yan, J. Stankovic, and T. Abdelzaher, "Analysis of target detection performance for wireless sensor networks," in *DCOSS*, 2005.

[5] O. Dousse, C. Tavoularis, and P. Thiran, "Delay of intrusion detection in wireless sensor networks," in *MobiHoc*, 2006.

[6] L. Lazos, R. Poovendran, and J. A. Ritcey, "Probabilistic detection of mobile targets in heterogeneous sensor networks," in *IPSN*, 2007.

[7] N. Bisnik, A. Abouzeid, and V. Isler, "Stochastic event capture using mobile sensors subject to a quality metric," in *MobiCom*, 2006.

[8] B. Liu and D. Towsley, "A study of the coverage of large-scale sensor networks," in *MASS*, 2004.

[9] P. Brass, "Bounds on coverage and target detection capabilities for models of networks of mobile sensors," *ACM Trans. Sen. Netw.*, vol. 3(2), 2007.

[10] M. F. Duarte and Y.-H. Hu, "Vehicle classification in distributed sensor networks," *J. Parallel and Distributed Computing*, vol. 64(7), 2004.

[11] D. Li, K. Wong, Y.-H. Hu, and A. Sayeed, "Detection, classification and tracking of targets in distributed sensor networks," *IEEE Signal Process. Mag.*, vol. 19(2), 2002.

[12] T. He, S. Krishnamurthy, J. A. Stankovic, T. Abdelzaher, L. Luo, R. Stoleru, T. Yan, L. Gu, J. Hui, and B. Krogh, "Energy-efficient surveillance system using wireless sensor networks," in *MobiSys*, 2004.

[13] M. Duarte and Y.-H. Hu, "Distance based decision fusion in a distributed wireless sensor network," in *IPSN*, 2003.
[14] T. Clouqueur, K. K. Saluja, and P. Ramanathan, "Fault tolerance in collaborative sensor networks for target detection," *IEEE Trans. Comput.*, vol. 53(3), 2004.
[15] X. Sheng and Y.-H. Hu, "Maximum likelihood multiple-source localization using acoustic energy measurements with wireless sensor networks," *IEEE Trans. Signal Process.*, vol. 53(1), 2005.
[16] D. Li and Y.-H. Hu, "Energy based collaborative source localization using acoustic micro-sensor array," *EUROSIP J. Applied Signal Processing*, no. 4, 2003.
[17] J. Kotecha, V. Ramachandran, and A. Sayeed, "Distributed Multitarget Classification in Wireless Sensor Networks," *IEEE J-SAC on Self-Organizing Distributed Collaborative Sensor Networks*, vol. 23(4), 2005.
[18] Z. Yuan, R. Tan, G. Xing, C. Lu, Y. Chen, and J. Wang, "Fast sensor placement algorithms for fusion-based target detection," in *RTSS*, 2008.
[19] R. Tan, G. Xing, J. Wang, and H. C. So, "Collaborative target detection in wireless sensor networks with reactive mobility," in *IWQoS*, 2008.
[20] ——, "Exploiting reactive mobility for collaborative target detection in wireless sensor networks," *IEEE Trans. Mobile Comput.*, 2009, IEEE Computer Society Digital Library.
[21] G. Xing, J. Wang, K. Shen, Q. Huang, X. Jia, and H. C. So, "Mobility-assisted spatiotemporal detection in wireless sensor networks," in *ICDCS*, 2008.
[22] R. Niu and P. K. Varshney, "Distributed detection and fusion in a large wireless sensor network of random size," *EURASIP J. Wireless Communication and Networking*, vol. 4, 2005.
[23] G. Xing, R. Tan, B. Liu, J. Wang, X. Jia, and C.-W. Yi, "Data fusion improves the coverage of wireless sensor networks," in *MobiCom*, 2009.
[24] M. Hata, "Empirical formula for propagation loss in land mobile radio services," *IEEE Trans. Veh. Technol.*, vol. 29, 1980.
[25] L. Gu, D. Jia, P. Vicaire, T. Yan, L. Luo, A. Tirumala, Q. Cao, T. He, J. Stankovic, T. Abdelzaher, and H. Bruce, "Lightweight detection and classification for wireless sensor networks in realistic environments," in *SenSys*, 2005.
[26] R. Tan, G. Xing, B. Liu, and J. Wang, "Impact of data fusion on real-time detection in sensor networks," Michigan State University, Tech. Rep., 2009, MSU-CSE-09-19.
[27] W.-P. Chen, J. C. Hou, and L. Sha, "Dynamic clustering for acoustic target tracking in wireless sensor networks," *IEEE Trans. Mobile Comput.*, vol. 3(3), 2004.
[28] P. Volgyesi, G. Balogh, A. Nadas, C. Nash, and A. Ledeczi, "Shooter Localization and Weapon Classification with Soldier-Wearable Networked Sensors," in *MobiSys*, 2007.
[29] B. P. Flanagan and K. W. Parker, "Robust distributed detection using low power acoustic sensors," The MITRE Corporation, Tech. Rep., 2005.

APPENDIX A.
DERIVING THE MEAN AND VARIANCE OF s_i

We first prove that $\{s_i|i \in \mathbf{F}_j\}$ are *i.i.d.* for any target position P. As sensors are deployed uniformly and independently, $\{d_i|i \in \mathbf{F}_j\}$ are *i.i.d.* for any P, where d_i is the distance between sensor i and point P. Therefore, $\{s_i|i \in \mathbf{F}_j\}$ are *i.i.d.* for any P, as s_i is a function of d_i, *i.e.*, $s_i = S \cdot w(d_i)$.

We then derive the mean and variance of s_i, *i.e.*, μ_s and σ_s^2. Let (x_p, y_p) and (x_i, y_i) denote the coordinates of point P and sensor i, respectively. The posterior PDF of (x_i, y_i) is $f(x_i, y_i) = \frac{1}{\pi R^2}$ where $(x_i - x_p)^2 + (y_i - y_p)^2 \le R^2$. Hence, the posterior CDF of d_i is given by $F(d_i) = \int_0^{2\pi} \mathrm{d}\theta \int_0^{d_i} \frac{1}{\pi R^2} \cdot x \mathrm{d}x = \frac{d_i^2}{R^2}$, where $d_i \in [0, R]$. Therefore,

$$\mu_s = \int_0^R S w(d_i) \mathrm{d}F(d_i) = \frac{2S}{R^2} \int_0^R w(d_i) d_i \mathrm{d}d_i,$$

$$\sigma_s^2 = \int_0^R S^2 w^2(d_i) \mathrm{d}F(d_i) - \mu_s^2 = \frac{2S^2}{R^2} \int_0^R w^2(d_i) d_i \mathrm{d}d_i - \mu_s^2.$$

By letting $\mu_0 = \frac{2}{R^2} \int_0^R w(d_i) d_i \mathrm{d}d_i$ and $\sigma_0^2 = \frac{2}{R^2} \int_0^R w^2(d_i) d_i \mathrm{d}d_i - \mu_0^2$, we have $\mu_s = S\mu_0$ and $\sigma_s^2 = S^2\sigma_0^2$.

APPENDIX B.
PROOF OF LEMMA 2

Proof: From Lemma 1 and Theorem 1, if the same α-delay of τ is achieved under the two models, we have

$$\mathbb{E}[P_D] = 1 - \mathrm{e}^{-\rho_d \pi r^2}. \tag{8}$$

We first prove the lower bound in (6). It is easy to verify that $P_D = Q(k\sqrt{N})$ is a concave function. According to Jensen's inequality, we have $\mathbb{E}[P_D] \le Q(k\sqrt{\mathbb{E}[N]}) = Q(k\sqrt{\rho_f \pi R^2})$. From (8), we have $1 - \mathrm{e}^{-\rho_d \pi r^2} = \mathbb{E}[P_D] \le Q(k\sqrt{\rho_f \pi R^2})$. Accordingly, $\rho_d \le -\frac{1}{\pi r^2} \ln \Phi(k\sqrt{\pi} R \cdot \sqrt{\rho_f})$, where $\Phi(x) = 1 - Q(x)$. Hence, the density ratio satisfies

$$\lim_{\tau \to 1^+} \frac{\rho_f}{\rho_d} \ge -\pi r^2 \cdot \lim_{\rho_f \to \infty} \frac{\rho_f}{\ln \Phi(k\sqrt{\pi} R \cdot \sqrt{\rho_f})} = \frac{2}{k^2 R^2} \cdot r^2.$$

In the above derivation, we use the equality $\lim_{x \to \infty} \frac{x}{\ln \Phi(\vartheta \sqrt{x})} = -\frac{2}{\vartheta^2}$, which can be verified via L'Hôpital's Rule (the proof can be found in [23]).

We now prove the upper bound in (6). As $P_D > 0$, according to Markov's inequality, for any given number c, we have

$$\mathbb{E}[P_D] \ge c \cdot \mathbb{P}(P_D \ge c). \tag{9}$$

We define ξ and c as follows:

$$\xi = \frac{k^2 + 2 - \sqrt{k^4 + 4k^2}}{2}, \quad c = Q(k\sqrt{\xi \rho_f \pi R^2}). \tag{10}$$

It's easy to verify that $\xi \in (0, 1)$. Therefore,

$$\mathbb{P}(P_D \ge c) = \mathbb{P}\left(Q(k\sqrt{N}) \ge Q(k\sqrt{\xi \rho_f \pi R^2})\right) = \mathbb{P}(N \ge \xi \rho_f \pi R^2).$$

As $N \sim \mathrm{Poi}(\rho_f \pi R^2)$ and the Poisson distribution approaches the normal distribution $\mathcal{N}(\rho_f \pi R^2, \rho_f \pi R^2)$ when $\rho_f \to \infty$, we have

$$\mathbb{P}(P_D \ge c) = Q\left(\frac{\xi \rho_f \pi R^2 - \rho_f \pi R^2}{\sqrt{\rho_f \pi R^2}}\right) = Q\left((\xi - 1)\sqrt{\rho_f \pi R^2}\right).$$

By replacing c and $\mathbb{P}(P_D \ge c)$ in (9), we have

$$\mathbb{E}[P_D] \ge Q\left(k\sqrt{\xi \rho_f \pi R^2}\right) \cdot Q\left((\xi - 1)\sqrt{\rho_f \pi R^2}\right).$$

It is easy to verify that $k\sqrt{\xi} = \xi - 1$. Thus the above inequality reduces to $\mathbb{E}[P_D] \ge Q^2(h\sqrt{\rho_f})$, where $h = k\sqrt{\xi \pi} R$. From (8), we have $1 - \mathrm{e}^{-\rho_d \pi r^2} = \mathbb{E}[P_D] \ge Q^2(h\sqrt{\rho_f})$. Accordingly, $\rho_d \ge -\frac{1}{\pi r^2} \cdot (\ln(1 + Q(h\sqrt{\rho_f})) + \ln \Phi(h\sqrt{\rho_f}))$. Hence, we have

$$\begin{aligned} \lim_{\tau \to 1^+} \frac{\rho_f}{\rho_d} &\le -\pi r^2 \lim_{\rho_f \to \infty} \frac{\rho_f}{\ln(1 + Q(h\sqrt{\rho_f})) + \ln \Phi(h\sqrt{\rho_f})} \\ &= -\pi r^2 \lim_{\rho_f \to \infty} \frac{\rho_f}{\ln \Phi(h\sqrt{\rho_f})} = \frac{2}{\xi k^2 R^2} \cdot r^2. \end{aligned} \tag{11}$$

Note that $h = k\sqrt{\xi \pi} R < 0$ and $\ln(1 + Q(h\sqrt{\rho_f})) = \ln 2$ when $\rho_f \to \infty$. We also use the aforementioned equality $\lim_{x \to \infty} \frac{x}{\ln \Phi(\vartheta \sqrt{x})} = -\frac{2}{\vartheta^2}$ to derive (11). ■